Genetic Algorithm-Based Identification Method of Thermal Parameters of the Power Electronic Devices Used in Renewable Energy Systems

Hanen Messaoudi* , Afef Bennani-Ben Abdelghani **‡ , Najiba Mrabet Bellaaj*** , Mohamed Orabi****

* Université de Tunis El Manar, Ecole Nationale d'Ingénieurs de Tunis LR11ES15 Laboratoire des Systèmes Electriques 1002, Tunis, Tunisia

**Université de Carthage, Institut National des Sciences Appliquées et de Technologie, 1080 Tunis Cedex, Tunisia

*** Université de Tunis El Manar, Institut Supérieur d'Informatique, 1002, Tunis, Tunisia

**** APEARC, Aswan University, Aswan, Egypt

(hanen.messaoudi@enit.utm.tn , afef.bennani@enit.utm.tn, najiba.bellaaj@isi.rnu.tn, orabi@ieee.org)

‡ Afef Bennani-Ben Abdelghani, 1080 Tunis Cedex, Tunisia, Tel: +216 20501005, afef.bennani@enit.utm.tn

Abstract- The electro-thermal RC networks are widely used in designing power semiconductor modules; in particular, those used in renewable energy systems for their health monitoring, reliability evaluation, lifetime estimation, and predictive maintenance. This paper proposes a new method based on the Genetic Algorithms (GAs) allowing the identification of the RC networks thermal parameters using the only information always available in all power devices datasheet which is the transient thermal impedance from the junction to the case $Z_{th(j-c)}$ curve. Thus, the proposed identification method doesn't require any extra information related to the power device's geometric structure or material properties or specific simulator and it doesn't include any complicated or time-consuming mathematical development or extensive derivation of analytical expressions. Simulation tests performed on Matlab simulator and experimental infrared results prove the accuracy and the effectiveness of the proposed GA-based identification method.

Keywords Genetic Algorithm (GA), Infrared (IR) camera, Junction temperature (T_j), solar inverter power modules, Thermal modelling, transient thermal impedance from junction to case ($Z_{th(j-c)}$).

1. Introduction

The Power electronic converters adapt flow of energy between the renewable energy generator such as wind turbines and solar panels; and the grid or stand-alone electric loads. The power semiconductor devices such as the IGBT modules are the basic components of the power converters and are the key for reliable renewable energy system [1]. The IGBTs Switch high currents that causes temperature fluctuations leading to a rapid deterioration of the device. Indeed, one of the important causes of power electronic failures, such as solder joint fatigue and bond wire fatigue, are temperature induced [2–4]. Thus, accurate monitoring of such thermal behavior is essential for forecasting the power device health status and remaining life. This would also help in avoiding unexpected catastrophic breakdowns of the whole renewable energy system.

The mostly used methods for estimating the thermal behavior of the power devices rely on estimating its junction temperature T_j. In practice there are three principal techniques actually used to measure the operating T_j of a power semiconductor device which are: the optical methods, the physically contacting methods and the electrical methods [5,6]. Each one of these three techniques has its limitations that drove the researchers to find better and easier alternatives. For instance, the optical methods require expensive, complicated, and time-consuming measuring equipment, such as the optical fibers, the infrared

microscopes, and the infrared cameras. Furthermore, these methods require visual and mechanical access to power devices, which is impossible for packaged power modules. Same issue for the physical contact methods that use the thermocouple [7] for example. However, for the electrical methods, there is no need to direct access to the device [6]. The T_j is then measured using only voltage and current probes on packaged power modules. The main disadvantage of the electrical methods is the fact that they only provide a representative average temperature and it's impossible to generate a temperature map.

Alternatively, typical electro-thermal models were proposed to estimate the T_j of packaged power modules [8–10]. The most widely used electro-thermal models in the datasheets are the RC Foster networks [11,12] because of their simplicity, time efficiency, and the ease of their integration into various circuit simulators such as PSIM and PLECS [7].

Multiple analytical and numerical methods have been reported in the literature for the parameterization of the power module thermal models. The Finite Element Method (FEM) is one of these methods that were extensively used due to its high accuracy. In [13] for instance, the authors developed a two dimensional (2D) thermal models equivalent to the heat equations discretization by the FEM and coupled to the electric model to provide an accurate IGBT model. The static and dynamic thermal behaviors of an IGBT mounted on a water-cooling heat sink were analyzed in [14] and the RC thermal parameters were extracted from the FEM results. Carubelli et al. reported in [15] a thermal modeling method for a multi-chip power module. The analytical functions of the thermal impedance of this module were established from the three-dimensional (3D) thermal simulations and experimental validation through direct chip temperature measurements. Additionally, a novel method was proposed in [16] for the extraction of an accurate thermal model of IGBT-based converter used for hybrid electric vehicles from the 3D FEM that has been calibrated by static experiments. In [17], a three phase IGBT inverter compact RC thermal model is presented. The R and C values in this work were identified according to the data extracted from the FEM model by FLOTHERM. In [18] also, the 3D FEM has been used for the identification of the thermal parameters of SiC IGBTs. The Finite Difference Method (FDM) was also used by Hefner for power IGBTs dynamic electro-thermal modeling [19].

The above-cited FEM-based and FDM-based identification methods have proved highly effective in terms of accuracy, however, they are time-consuming, they employ specific commercial simulators, and they require the knowledge of the device's geometric structure and materiel properties which may not be available.

Otherwise, multiple methods that relied on the experimental curves provided in the device's datasheet were proposed to extract the thermal parameters of power modules. In [20] and [7] for example, the authors proposed a computationally efficient method based on numerical analysis and exponential fitting of the experimental $Z_{th(j-c)}$ curve to generate the thermal model of an IGBT module. The junction temperature cooling curve has also been used for the same purpose [21-23]. K.Gorecki et al. also proposed an identification method using the ESTYM program [24]. This program relies on an algorithm allowing the estimation of thermal resistance values R_{th} by averaging the $Z_{th(j-c)}$ waveform in the steady-state, and the time constant values τ_i by the least square method. However, these methods contain multiple complex mathematical developments with extensive derivations and integrations, and they are restricted by constant or accurate loss models. Another identification method based on numerical analysis by deconvolution was firstly introduced in [25] and widely used in [26,27]. However, this method is not always convergent, and it lacks accuracy. In [28] the proposed method includes physics-based analysis and uses structural and material data to extract the thermal parameters and it requires complicated and time-consuming analysis. Recent research works proposed a quasi-online identification method using the relationship between the time constants of the T_j cooling curve and the thermal parameters of the IGBT module [8,22,29]. The advantage of this method is the ability to accurately estimate the parameters considering the aging procedure of the device. However, it requires complicated mathematical development. Some research works treat the problem of the extraction of the thermal models as an optimization problem and they proposed direct multi-exponential curve fitting methods using EXCEL optimizer [30] or classical optimization techniques like the least square error technique on MATLAB software [31,32].

In this paper, a novel method based on the Genetic Algorithms (GA) optimization techniques is proposed. The GA is a robust algorithm that carries out a global search using probabilistic rules and not deterministic ones [33,34]. The GA optimization method has been used in different renewable energy systems issues such as the partial shading, the power quality issue, and the battery energy management [35-39].

The major strengths of the proposed GA-based method are the fact that it does not require any information related to the power device, only the $Z_{th(j-c)}$ curve which is always available in the datasheet is needed, unlike the FEM-based simulations, for instance. Furthermore, it's independent of the device package type and the number of the RC branches, it doesn't include complicated or time-consuming mathematical development such as in [8,22,29-30], and doesn't require special simulation platforms as in [40,41].

Simulation tests using a 0.6 kV IGBT module from INFINEON have been performed to prove the effectiveness of the proposed GA-based method. The thermal parameter values of the considered IGBT module are provided in its datasheet. Thus, they were compared with the estimated ones using the proposed method, and they are found to be in excellent agreement. Furthermore, the proposed method has been experimentally validated using an infrared camera.

This paper is organized as follows: In section 2, the thermal modelling of power devices is presented. Then, the proposed GA-based identification method is introduced and detailed in section 3. In section 4 the simulation tests are detailed and the results proving the efficiency of the proposed method are depicted. Finally, the experimental steps and results to validate the proper operation of the proposed method are presented in section 5.

2. Power semiconductor thermal modelling

Many emerging and important energy conversion applications such as renewable energies, traction, electric vehicles, etc., involve power electronics as essential parts, which need to fulfill a relatively large amount of power. As the switching frequency and the power density are important inside these conversion applications, as well as the high cost of failures, which are mostly temperature-induced [4,42], the thermal analysis of power electronics switching systems becomes a crucial task. This analysis will afford helpful information about the performance and the reliability of the power semiconductor. Traditionally, dynamic thermal resistance-capacitance (RC) networks that represent an equivalent heat transfer from the power device's chip to the heat sink are widely used for thermal analysis [43,44]. These networks are commonly described by either a Foster [25,43], or a Cauer [45,46] model. Fig. 1 shows the structure of an RC Cauer network (a) and an RC Foster network (b).
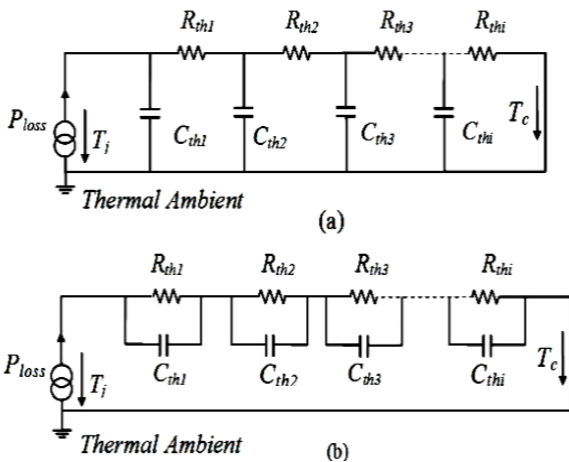

Fig. 1. Cauer thermal model (a) and Foster thermal model (b) topologies.

These thermal networks are simple, time-efficient, and can be easily integrated into various circuit simulators such as PLECS, Spice, and PSIM [7]. Both network constructions are equivalent from the point of view of T_j. However, the Cauer model also named the T model, represents the internal physical structure of the power device layers [47], i.e., the number of RC branches is equal to the number of the physical layers of the device. Thus, each RC branch is assigned to a physical layer and each node represents a real temperature [48], which makes it computationally complex to implement. By contrast, the Foster network has no direct physical interpretation, and it cannot provide temperature

changes in the internal layers of the device. This model is easier to implement, is widely used in power device datasheets, and can be extracted according to IEC standard 60747-96.3.13 [47]. It has been proven that four RC branches may describe sufficiently well the thermal behavior of a power semiconductor device [46]. Moreover, the time constants in the Foster model are equal to the product of each RC of each branch separately Rthi× Cthi, where i is the number of the RC branches. But in the Cauer model, each time constant is a function of all the resistances and capacitances of the circuit which makes its calculation complicated. In this paper, a four-order Foster RC network was used. The thermal RC network parameters R_{thi} and C_{thi}, (i = 1..4) are in some cases given in the device datasheet in tabular form as R_{th} (or r) and (τ: the time constant) pairs, as shown in the example of the IGBT module F3L50R06W1E3_B11 in Fig. 2.

Fig. 2. Foster network RC thermal parameters of the IGBTs of the F3L50R06W1E3_B11 (600 V/50 A) [49].

However, some power semiconductor manufacturers do not provide these values; they only afford the transient thermal impedance from the junction to the case $Z_{th(j-c)}$ curve. This curve presents the transient response of a peak temperature to an applied step of constant power. Figure 3 shows an example of a $Z_{th(j-c)}$ curve of the IGBT module SKM50GB12T4 provided in its datasheet.

The transient thermal impedance from the junction to the case of a power device is governed by Eq. (1), where n is the number of the RC branches of the network:

$$Z_{th(j-c)}(t) = \sum_{i=1}^{n} R_{thi} \times (1 - e^{\frac{-t}{\tau_i}})$$ (1)
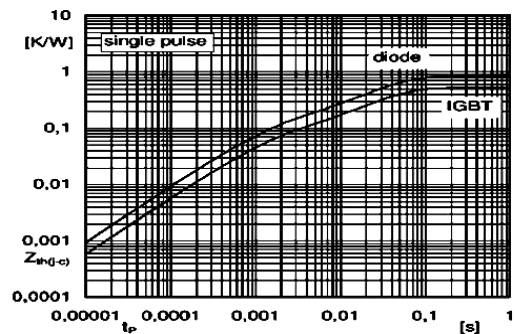

Fig. 3. Thermal impedance curve of the IGBT module SKM50GB12T4 (1200 V/62 A) [50].

3. Proposed GA-based identification method

Identifying the thermal parameters from only the $Z_{th(j-c)}$ curve, which is always available in the device datasheet with no extra information about the device's geometric structure

or material properties is a challenging task. This identification issue consists on the resolution of a non linear and mathematical complex eight parameter equation $Z_{th}=f(R_{th1}, R_{th2}, R_{th3}, R_{th4}, C_{th1}, C_{th2}, C_{th3}, C_{th4})$. In this paper, the GA optimization technique is preferred to solve this problem as it's one of the well-documented and mature optimization algorithms.

3.1. Genetic algorithm

The GA is a robust and flexible technique inspired by biological evolution and is used to solve complex optimization problems [34,51]. It deals with encoding parameters and not the parameters themselves, and it investigates the search domain through a population of solutions and not a single one. Furthermore, the GA detects the global minimum of fitness rather than a local solution unlike the traditional optimization methods that search from a single point, and it was successfully used to model parameters optimization and power system dispatches[52], [53]. Also, in contrast to the conventional optimization techniques, the GA needs neither to differentiate an objective function with many mathematical requirements nor to start with a good initial estimate. The GA fulfills a selection process using genetic operators such as selection, crossover, and mutation, which allows the fittest parameters to survive, and it eliminates the least fit ones. Accordingly, the use of the GA technique can avoid intensive computations, which are usually found in stochastic optimization techniques.

3.2. Problem formulation

For this work, the MATLAB GA Optimization Toolbox was used. The GA approach is the same for any application. Only a few parameters have to be set for the algorithm to turn on. To optimize the function $Z_{th}=f(R_{th1}, R_{th2}, R_{th3}, R_{th4}, C_{th1}, C_{th2}, C_{th3}, C_{th4})$ using the GA and since this latter requires good initial ranges rather than precise initials of the parameters, each parameter is firstly coded as a binary or a real string of length. For the actual work, a real string encoding is preferred, and each parameter is limited between a max and min value chosen randomly, e.g.

$$R_{thi} = [min_{Rthi} .. max_{Rthi}]$$
$$C_{thi} = [min_{Cthi} .. max_{Cthi}]$$

In this work, the min and max values were chosen randomly in the same range as some other IGBT modules whose values are available in their datasheets. The set $f(R_{th1}, R_{th2}, R_{th3}, R_{th4}, C_{th1}, C_{th2}, C_{th3}, C_{th4})$ is called chromosome and the R_{thi} and the C_{thi} are the genes, i = 1..4. The principle of a basic GA cycle is described step by step by the flowchart depicted in Fig. 4 with the following operations:

1) Generating the initial population;
2) Performance evaluating;
3) Fitness calculation;
4) Selection;
5) Crossover;
6) Mutation;
7) Reinsertion.

And it's running as follows:

1) Select the real-coded chromosomes. Each chromosome contains eight parameters or genes.

2) Initialize the population and set its size: a large population size might increase the rate of convergence; however, it also increases the calculation time. Hence, the selection of an optimum population size needs some experience in GA. In general, it can be defined as 5 to 10 times the problem dimension. The population is initialized with randomly chosen minimum and maximum values of the thermal parameters.
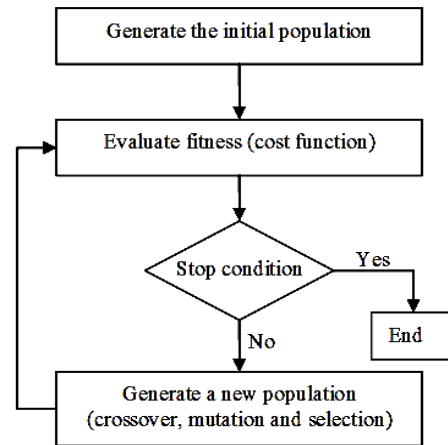

Fig. 4. GA basic cycle.

3) The fitness of each chromosome is evaluated through a cost function. The objective of this optimization study is to identify the RC parameters that allows the reproduction of the evolution of the $Z_{th(j-c)}$ curve of the considered power module; accordingly, the cost function has been chosen as the Mean Square Error (MSE) between the real $Z_{th(j-c)}$ curve and the estimated one, which guarantees a good accuracy. The estimated curve is calculated by the Eq. (1) using the estimated thermal parameters by the proposed GA-based identification method. This curve is compared to a real $Z_{th(j-c)}$ curve, which is the input of the algorithm. The real curve is either given in the device datasheet or is the curve affected by the aging process calculated after an excessive operation of the device.

4) Usually, the GA runs for a fixed number of iterations to find a solution. In each iteration, the chromosomes are selected based on their fitness value. Then they go through crossover where a new offspring is created using part of the chromosome genes, and mutation performed by changing one of the genes in a random way. Thus, a new population is determined, and it goes through the same cycle starting from the evaluation of the fitness value.

5) The GA stops when a stopping criterion is met. In this work, the algorithm detects if there is no changes in the best fitness values during a period of time indicated by the Matlab command **'stall time limit'** given in seconds. The default value of this parameter is about 20 s and it can be changed by the user in the

Stopping criteria options in the **Genetic Algorithm Toolbox** of Matlab.

The GA parameters in this work are initially set as follow:

- ➤ Initial population size = 100;
- ➤ Number of iteration = 50;
- ➤ Probability of crossover = 0.8;
- ➤ mutation probability = 0.001;

3.3. Simulation results

For the simulation tests performed on MATLAB the IGBT module F3L50R06W1E3_B11 (600 V/50 A) from INFINEON is considered because its thermal parameter values are available on its datasheet. The F3L50R06W1E3_B11 module is a three-level Neutral Point Clamped (NPC) converter, made by four IGBTs with their anti-parallel diodes and two clamp diodes. The proposed GA-based method identifies the thermal parameters of the IGBTs and the diodes of the module separately. Table 1 illustrates the estimated values $\hat{R}_{thi}$ and $\hat{\tau}_i$ and the real ones R_{thi} and τ_i, (i = 1...4), which are the experimental values depicted in the datasheet.

Table 1. Real and estimated values of the F3L50R06W1E3_B11 IGBTs thermal parameters

i	1	2	3	4
R_{thi} (K/W)	0.083	0.193	0.586	0.588
$\hat{R}_{thi}$ (K/W)	0.104	0.171	0.717	0.458
τ_i (s)	0.0005	0.005	0.05	0.2
$\hat{\tau}_i$ (s)	0.0007	0.005	0.057	0.23
Mean squared error of the Z_{th} estimation		7.10^{-3}		

The estimated values are later used to calculate the estimated transient thermal impedance curve. This curve and the experimental one $Z_{th(j-c)}$ provided in the datasheet are represented in Fig. 5.
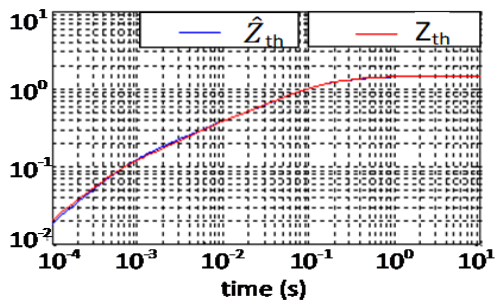

Fig. 5. Estimated and real transient thermal impedance curves of the IGBTs of the F3L50R06W1E3_B11 module.

Similarly, the estimated and the real thermal parameters values (datasheet values) of the inverse diodes and the clamp diodes of the considered module are depicted in Table 2 and Table 3, respectively.

Table 2. Real and estimated values of the F3L50R06W1E3_B11 inverse diodes thermal parameters.

i	1	2	3	4
R_{thi} (K/W)	0.157	0.337	0.758	0.598
$\hat{R}_{thi}$ (K/W)	0.195	0.284	0.839	0.532
τ_i (s)	0.0005	0.005	0.05	0.2
$\hat{\tau}_i$ (s)	0.0006	0.005	0.048	0.264
Mean squared error of the Z_{th} estimation		$5,6.10^{-2}$		

Table 3. Real and estimated values of the F3L50R06W1E3_B11 clamp diodes thermal parameters

i	1	2	3	4
R_{thi} (K/W)	0.118	0.26	0.617	0.505
$\hat{R}_{thi}$ (K/W)	0.141	0.379	0.638	0.34
τ_i (s)	0.0005	0.005	0.05	0.2
$\hat{\tau}_i$ (s)	0.0005	0.00399	0.07	0.24
Mean squared error of the Z_{th} estimation		7.10^{-3}		

Figure 6 and Figure 7 illustrate the estimated and real transient thermal impedance curve for the inverse diodes and the clamp diodes, respectively.
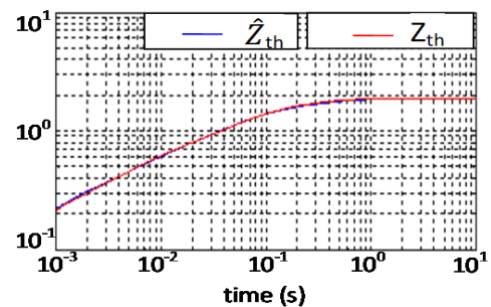

Fig. 6. Estimated and real transient thermal impedance curve of theF3L50R06W1E3_B11 inverse diodes.
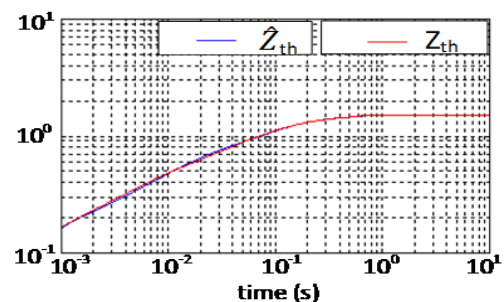

Fig. 7. Estimated and real transient thermal impedance curve of theF3L50R06W1E3_B11 clamp diodes.

According to Fig. 5, Fig. 6, and Fig. 7 the estimated and the experimental transient thermal impedance curves of the IGBTs, the inverse and the clamp diodes are nearly superimposed, especially at the steady-state.

Moreover, in Table 1, Table 2, and Table 3 the exact value of the mean squared error between the the estimated and the experimental transient thermal impedance curves of

the IGBTs, the inverse diodes, and the clamp diodes are about 7.10^{-3}, $5,6.10^{-2}$, and 7.10^{-3}, respectively. The low values of these errors further prove the effectiveness and the accuracy of the proposed GA-based identification method.

3.4. Accuracy evaluation and Discussion

In order to prove the accuracy and the usefulness of the proposed GA-based identification method, it was compared with some other identification methods reported in the literature, which are the FEM-based method reported in [54], the proposed method based on the cooling curve of junction temperature in [22] and the JESD51-14 method presented in [56]. Table 4 depicts the comparison results between the thermal parameters identified using the GA-based method and the FEM-based one of a 600 V/150 A Fuji U-series dual-pack IGBT module.

Table 4. Experimental and estimated thermal parameters values by the FEM-based method and the GA-based method [54].

Thermal parameters	Experimental values	GA	FEM
R_{th1} (°C/W)	0.0084	0.0078	0.0223
R_{th2} (°C/W)	0.0041	0.0011	0.2344
R_{th3} (°C/W)	0.2142	0.127	0.0004
R_{th4} (°C/W)	0.0233	0.0107	0.0155
τ_1 (s)	0.0036	0.003	0.00403
τ_2 (s)	0.000009	0.0000055	0.0833
τ_3 (s)	0.0533	0.044	0,000033
τ_4 (s)	0.0034	0.0035	0.0832

Table 5 shows the comparison results between the experimental values provided in the datasheet, and those identified using the GA-based method, the cooling curve-based method, and the JESD51-14 method of the IGBTs of the IGBT module FF50R12RT4.

According to the results presented in Table 4, it can be clearly observed that the gap between the estimated values using the proposed method and the experimental values is very small and it reaches approximately less than 25%. However, the gap between the values estimated using the FEM-based method and the experimental ones is very large and it reaches more than 90%. Thus, this comparison attests very well to the effectiveness and the accuracy of the GA optimization technique over the FEM-based ones. The results depicted in Table 5 shows that the use of the proposed GA-based method decreases the gap between the experimental values from the datasheet and the estimated ones by almost 30%.

Table 5. Experimental and estimated thermal parameters values by the Cooling Curve (CC)-based method, the JESD51-14-based method, and the GA-based method

Thermal parameters	Experimental values	GA	CC	JESD51-14
R_{th1} (°C/W)	0.0318	0.0166	0.075	0.08
R_{th2} (°C/W)	0.1749	0.156	0.212	0.2
R_{th3} (°C/W)	0.1696	0.1872	0.24	0.235
R_{th4} (°C/W)	0.1537	0.0905	--	--
τ_1 (s)	0.0099	0.0095	0.0075	0.0076
τ_2 (s)	0.0199	0.0221	0.0154	0.014
τ_3 (s)	0.0499	0.0365	2.364	2.311
τ_4 (s)	0.099	0.0743	--	--

4. Experimental validation and discussion

The experimental test bench depicted in Fig. 8 was installed in the laboratory to verify the effectiveness of the proposed GA-based identification method.
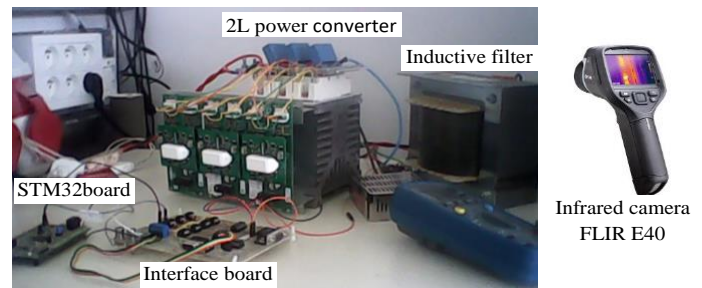

Fig. 8. Experimental test bench with infrared camera.

The experimental test bench specification details are shown in Table 6.

Table 6. Experimental test bench specification details

Component	Characteristics
Power converter switches	SKM50GB1 2T4, 1200 V, 50 A
Adjustable resistive load	Up to 2,5 kW
L filter	60 mH
Digital target	STM32F4 DISCOVERY

The converter is made of three SKM50GB12T4IGBT modules for each leg and is mounted on a heat sink with a thermal resistance R_{ths}= 0.33 K/W. The gate signals of the converter power switches are generated by a classical carrier-based Pulse Width Modulation (PWM) strategy through an STM32 board. The ultra-fast IR camera FLIR E40 [56] was used for temperature monitoring.

The 2L converter is shown in Fig. 9. Each converter leg is made by the IGBT module SKM50GB12T4, which is the device under test. The SKM50GB12T4 module contains two IGBTs and two inverse diodes.

The gate signals C_i (i =1..6) of the six IGBTs are generated using a Pulse Width Modulation (PWM) implemented in the STM23F4DISCOVERY board. The switching frequency is f_{sw} = 10 kH.
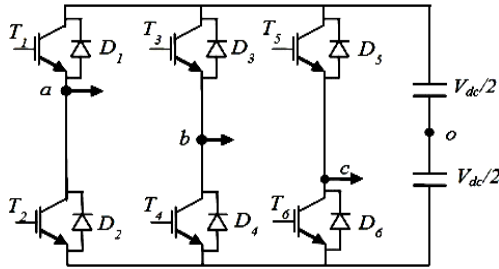
Fig. 9. Two level converter topology.

4.1. Experimental setup

Only the first leg of the converter is considered. The principle of the experimental validation is to compare the temperatures of the converter leg estimated through a thermal model elaborated using the thermal parameters estimated by the GA-based method with those measured by an infrared camera.

The procedure of the experimental test is as follow:

1) The estimation of the thermal parameters (R_{thi} and τ_i, (i = 1..4 and $\tau_i = R_{thi} \times C_{thi}$)) of the converter leg devices (two IGBTs T_1 and T_2 and two diodes D_1 and D_2) using the proposed GA-based method. The estimated parameters of the IGBTs and the diodes are depicted in Table 7 and Table 8, respectively.

Table 7. Estimated R_{thi} and τ_i values of the SKM50GB12T4 IGBTs.

i	1	2	3	4
R_{thi} (K/W)	0.0392	0.1512	0.1514	0.1882
τ_i (s)	0.001	0.0078	0.224	0.12

Table 8. Estimated R_{thi} and τ_i values of the SKM50GB12T4 diodes.

i	1	2	3	4
R_{thi} (K/W)	0.1167	0.2287	0.2289	0.2657
τ_i (s)	0.0022	0.008	0.023	0.024

The resulting thermal impedance curves drawn using the estimated parameters depicted in Table 7 and Table 8 are shown in Fig. 10.
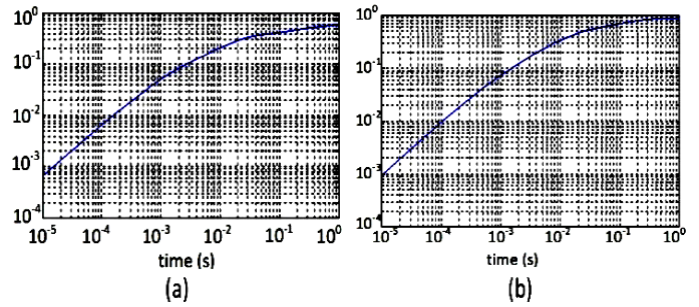

Fig. 10. Estimated transient thermal impedance curve of the SKM50GB12T4 IGBT (a) and diode (b).

Compared to the manufacturer's curves shown in Figure 3, the estimated curves calculated by Eq. (1) using the estimated parameters and depicted in Fig. 10 are nearly superimposed, which further proves the effectiveness of the proposed GA-based identification method.

2) The elaboration of the thermal model of the converter leg using the thermal parameters estimated in step 1. Figure 11 presents the elaborated thermal model.
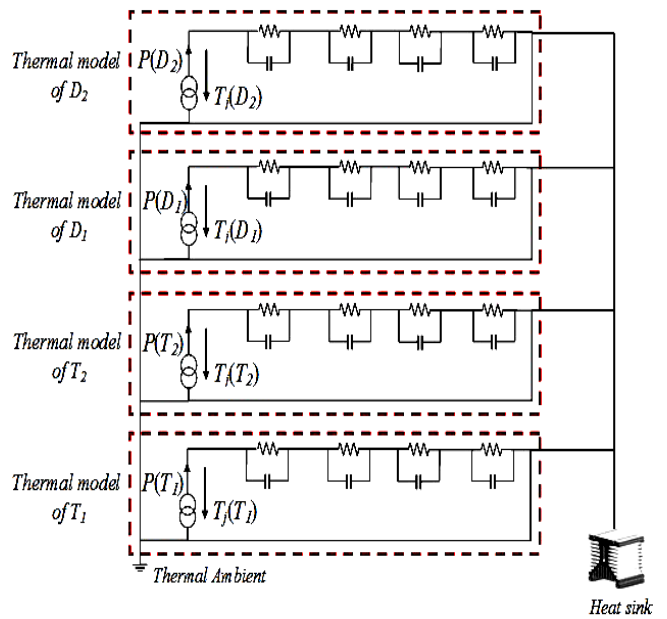

Fig. 11. Thermal model of the SKM50GB12T4 IGBT module from SEMIKRON.

The inputs of this model are the total power losses dissipated in the two IGBTs P_{tot_Ti} and the two diodes P_{tot_Di}, (i = 1...2). The total losses of a power device are the sum of its switching P_{sw} and conduction P_{cond} losses (Eq. 2):

$$\mathrm{P}_{tot} = P_{sw} + P_{cond} \tag{2}$$

The conduction and switching losses calculation are governed by Eq. 3 and Eq. 4, respectively.

$$P_{cond} = \frac{1}{T_{sw}} \int_0^{T_{sw}} (V_k \times I_k(t)) dt \tag{3}$$

$$P_{sw} = (E_{on} + E_{off} + E_{rr}) \times f_{sw} \qquad (4)$$

Where $T_{sw} = \dfrac{1}{f_{sw}}$ is the switching period, f_{sw} is the switching frequency, V_k is the voltage across the power device (IGBT or diode), I_k is the current through the device, E_{on}, E_{off} and E_{rr} are respectively, the consumed energy at the turning ON, the consumed energy at the turning OFF, and the consumed energy at the reverse recovery phase.

3) This thermal model was elaborated on the PSIM simulator and it serves to estimate the junction temperature of each device of the converter. T_{j_Ti} and T_{j_Di}, (i = 1..2) are, respectively, the junction temperatures of the IGBTs and diodes.

4) The estimation of the power module case temperature T_c measured on the package outside surface. This step is very important since in practice the junction temperatures T_j of the elementary power devices inside the modern packaged IGBT module are not accessible. T_c is a function of the T_j, the total dissipated losses and the transient thermal impedance from junction to case and is governed by Eq. (5).

$$T_c(t) = T_j(t) - P_{tot} \times Z_{th(j-c)}(t) \qquad (5)$$

In the following, four operating points O_{pi} for i = 1...4 of the concerned leg of the 2L power converter with the converter results are detailed in Table 9.

Table 9. Operating point details.

	O_{p1}	O_{p2}	O_{p3}	O_{p4}
V_{DC} (V)	100	100	300	120
Duty cycle (α)	0.2	0.8	0.2	0.8
I_{out} (A)	1.3	5.25	4.6	7.4
P (W)	26	420	888	1380
Estimated T_c (°C)	29.3	31.97	32.2	42.9
Experimental T_c (°C)	29.7	32.7	33.5	42.5

The estimated junction and case temperature distributions inside the converter leg for each operating point are shown in Figure 12.

The estimated case temperatures T_c shown in Fig. 12 are the case temperatures corresponding to the IGBT T_1 and the IGBT T_2. It reaches about 29.3 °C for the operating point O_{p1}, 31.97 °C for O_{p2}, 2.9°C for O_{p3}, and 42.9 °C for O_{p4}.

Later, these simulation results will be compared to the experimental ones. In fact, only the case temperatures can be experimentally monitored by an infrared camera, since practically it's impossible to access to the internal junction temperatures of a packaged IGBT module.
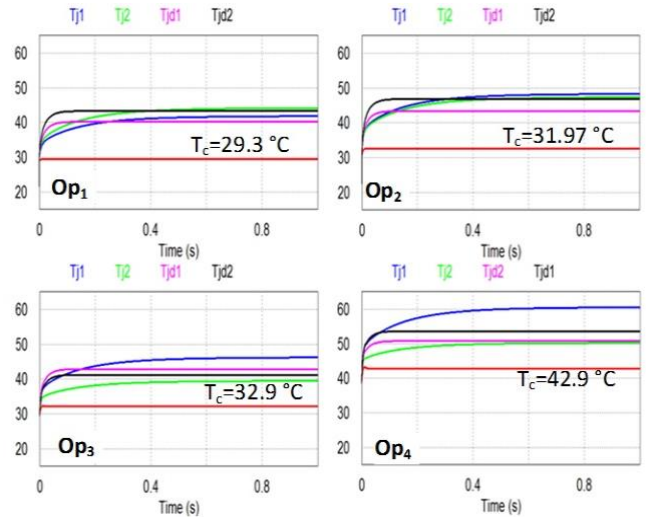

Fig. 12. Junction and case temperatures distribution.

5) Compare the calculated T_c with the experimental ones measured using the infrared camera and depicted in Fig. 13. Only the case temperatures are monitored by the infrared camera since it's impossible to measure the internal junction temperature of the package power module devices.

4.2. Experimental results

The infrared emission technique is based on the radiation emitted by solids at infrared frequencies. Its major advantage is that it does not perturb the device under test. The adopted infrared camera is characterized by a high-resolution 3.2 Megapixels digital camera with a high temperature range from -20 °C to 600 °C and high sensitivity (< 0,07 °C at 30 °C). In real-time mode, the camera has an adjustable frame rate of 60 Hz. Furthermore, it can be controlled by a computer or a Smartphone through a USB port, Wi-Fi or Bluetooth, so that the infrared pictures and data can be recorded.

Figure 13 shows the converter input voltage V_{dc}, the output voltage V_{out} and current I_{out} obtained for the operating point O_{p3} and for a resistive load R = 70 Ω.
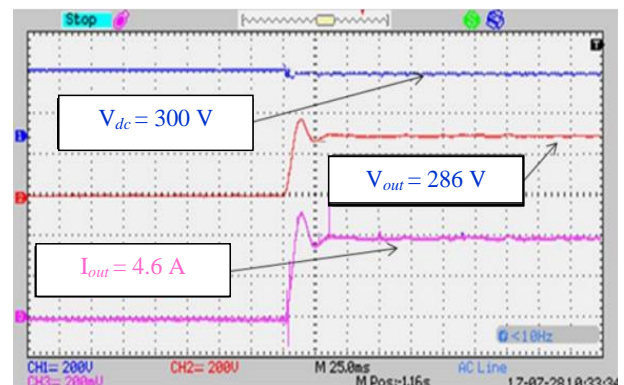

Fig. 13. Converter operating results

The experimental maximum T_c measured by the infrared camera for each operating point is shown in Fig. 14. The maximum T_c depicted in Fig. 13 are about 29.7°C for the operating point O_{p1}, 32.7 °C for O_{p2}, 33.5 °C for O_{p3}, and 42.5 °C for O_{p4}. Compared with the results depicted in Fig. 12, it's observed that these experimental measurements are nearly similar to the simulation ones, which further proves the efficiency of the proposed GA-based method for the identification of the thermal model parameters.
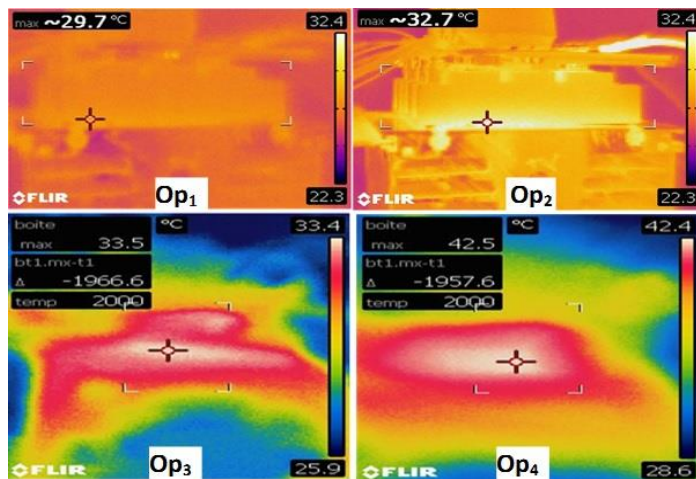

Fig. 14. Case temperature pictures captured by the infrared camera.

4.3. Future works

The intended future works consist of considering the aging procedure of the power devices by applying an aging test to monitor its influence on the transient thermal impedance waveform and obviously on the case temperature distribution and to verify the accuracy of the proposed GA-based method during the test. The aging test consists of applying a very high pulsed-current during small periods. The whole operation needs almost 20000 power cycles of about 10 seconds before the IGBT reaches a fatigue stage [57] and almost 40000 power cycles for the collector-emitter saturation voltage to increase15% over its nominal value, and the IGBT, in this case, is considered in severe degradation [58]. Furthermore, the increase of the operating current will enhance the mutual thermal coupling between the module devices. Thus, this phenomenon must be considered in these future works, since it impacts the transient thermal impedance evolution, which is the main input of the proposed GA-based method. An example of a proposed method for the measurement of the self and mutual $Z_{th(j-c)}$ curve of an IGBT module and the identification of the corresponding thermal parameters was reported in [59].

5. Conclusion

Reliability of power electronic devices and obviously of the renewable energy systems could be described as the ability to perform their desired functions, under declared conditions, for a predetermined period of time. However, the main causes of their failure are temperature induced.

Therefore, the monitoring of the device thermal behavior is crucial to predict its health status.

A new method based on the GA technique for the estimation of power IGBT modules thermal model parameters is proposed in this paper. Unlike numerous identification methods reported in the literature, the proposed GA-based method allows the estimation of the thermal parameters without any prior knowledge of the device, only the device's transient thermal impedance curve $Z_{th(j-c)}$, which is always available in the power module datasheet, is needed. The efficiency of the proposed method has been proved firstly by simulations and then experimentally validated through a low voltage test bench containing a three-phase two-level power converter with an ultra-fast IR camera for temperature monitoring. The accuracy of the proposed method has been also evaluated through a comparison with some other effective methods reported in the literature. The results reported in this paper confirm that the GA optimization technique is quick, robust, powerful, efficient, and easily implemented on MATLAB software and does not require special simulation platforms or software.

References

[1] U. M. Choi, K. B. Lee and F. Blaabjerg, "Power electronics for renewable energy systems: Wind turbine and photovoltaic systems", International Conference on Renewable Energy Research and Applications (ICRERA), pp. 1-8, 2012. (Conference Paper)

[2] J. Ortizgonzalez and O. Alatise, "Bias Temperature Instability and Junction Temperature Measurement Using Electrical Parameters in SiC Power MOSFETs", IEEE Transactions on Industry Applications, DOI: 10.1109/TIA.2020.3045120, vol. 57, no 2, pp. 1664-1676, 2020. (Article)

[3] L. Peng, W. Shen, A. Feng, Y. Liu, D. Gao, H. Yan, and F. Wu, "Method for obtaining junction temperature of power semiconductor devices combining computational fluid dynamics and thermal network", Nuclear Instruments and Methods in Physics Research Section A: Accelerators, Spectrometers, Detectors and Associated Equipment, vol. 976, p. 164260, 2020. (Article)

[4] Y. Li, Z. Chen, J. Li and C. Guo, "Junction Temperature Measurement of IGBT in Accelerated Degradation Test", the International Workshop on Electronic Communication and Artificial Intelligence (IWECAI), Shanghai, China, pp. 1-5, 2020. (Conference Paper)

[5] S. M. Sze, Y. Li, and K. K. Ng, "Physics of semiconductor devices", John wiley & sons, 2021. (Book)

[6] M. Y. Wang, G. Q. Lu, Y. H. Mei, X. Li, L. Wang, and G. Chen, "Electrical method to measure the transient thermal impedance of insulated gate bipolar transistor module", IET Power Electronics, DOI: 10.1049/iet-pel.2014.0120, vol. 8, no 6, pp. 1009-1016, 2015. (Article)

[7] Z. Luo, H. Ahn and M. A. E. Nokali, "A thermal model for insulated gate bipolar transistor module", IEEE Transactions on Power Electronics, DOI: 10.1109/TPEL.2004.830089, vol. 19, no 4, pp. 902-907, 2004. (Article)

[8] X. Du, X. Du, J. Zhang, and G. Li, "Numerical junction temperature calculation method for reliability evaluation of power semiconductors in power electronics converters", the Journal of Power Electronics, DOI: 10.1007/s43236-020-00154-z, vol. 21, no 1, pp. 184–194, 2021. (Article)

[9] P. Górecki and K. Górecki, "Non-linear compact thermal model of IGBTs", 21st European Microelectronics and Packaging Conference (EMPC) & Exhibition", Warsaw, pp. 1-5, 2017. (Conference Paper)

[10] P. Górecki, K.Górecki, and J. Zarebski, "Thermal model of the igbt module, in Journal of Physics", Journal of Physics: Conference Series, vol. 1033, no 1. IOP Publishing, p. 012001, 2018. (Article)

[11] M. Xu, K. Ma, B. Liu and X. Cai, "Modelling and Correlation of Two Thermal Paths in Frequency-domain Thermal Impedance Model of Power Module", IEEE Journal of Emerging and Selected Topics in Power Electronics, DOI: 10.1109/JESTPE.2020.3034574, vol. 9, no 4, pp. 3971-3981, 2020. (Article)

[12] H. Chen, B. Ji, V. Pickert and W. Cao, "Real-Time Temperature Estimation for Power MOSFETs Considering Thermal Aging Effects", IEEE Transactions on Device and Materials Reliability, DOI : 10.1109/TDMR.2013.2292547, vol. 14, no 1, pp. 220-228, 2014. (Article)

[13] A. Ammous, K. Ammous, H. Morel, B. Allard, D. Bergogne, F. Sellami, and J. P. Chante, "Electrothermal modeling of IGBTs: application to short-circuit conditions", IEEE Transactions on Power Electronics, DOI : 10.1109/63.849049, vol. 15, no 4, pp. 778-790, 2000. (Article)

[14] C-S. Yun, P. Malberti, M. Ciappa and W. Fichtner, "Thermal component model for electro-thermal analysis of IGBT module systems", IEEE Transactions on Advanced Packaging, DOI : 10.1109/6040.938309, vol. 24, no 3, pp. 401-406, 2001. (Article)

[15] S. Carubelli and Z. Khatir, "Experimental validation of a thermal modelling method dedicated to multichip power modules in operating conditions", Microelectronics journal, DOI: 0.1016/S0026-2692(03)00205-2, vol. 34, no 12, pp. 1143-1151, 2003. (Article)

[16] M. Ciappa, W. Fichtner, T. Kojima, Y. Yamada, and Y. Nishibe, "Extraction of accurate thermal compact models for fast electro-thermal simulation of IGBT modules in hybrid electric vehicles", Microelectronics Reliability, vol. 45, no 9-11, pp. 1694-1699, 2005. (Article)

[17] Z. Zhou, P. M. Holland and P. Igic, "Compact thermal model of a three-phase IGBT inverter power module", the 26th International Conference on Microelectronics, pp.67-170, 2008. (Conference Paper)

[18] A. Nejadpak, A. Nejadpak and O. A. Mohammed, "A physics-based, dynamic electro-thermal model of silicon carbide power IGBT devices", the 28th Annual IEEE Applied Power Electronics Conference and Exposition (APEC), Long Beach, CA, USA, pp.201-206, 2013. (Conference Paper)

[19] A. R. Hefner, "A dynamic electro-thermal model for the IGBT", IEEE Transactions on Industry Applications, DOI : 10.1109/28.287517, vol. 30, no 2, pp. 394-405, 1994. (Article)

[20] M. Jin and X. Fu, "A mathematical method of generating thermal models for power devices", the 2nd International Conference on Mechanical and Electronics Engineering, Kyoto, Japan, vol. 1, pp. V1-142-V1-145, 2010. (Conference Paper)

[21] J. V. Gragger, C. J. Fenz, H. Kernstock and C. Kral, "A fast inverter model for electro-thermal simulation", the 27th Annual IEEE Applied Power Electronics Conference and Exposition (APEC), Orlando, FL, USA, pp. 2548-2555, 2012. (Conference Paper)

[22] X. Du, T. Li, J. Zhang, H. Tai, P. Sun and L. Zhou, "Thermal network parameter identification of IGBT module based on the cooling curve of junction temperature", IEEE Applied Power Electronics Conference and Exposition (APEC), Long Beach, CA, USA, pp. 2992-2997, 2016. (Conference Paper)

[23] X. Du, J. Zhang, S. Zheng and H. Tai, "Thermal Network Parameter Estimation Using Cooling Curve of IGBT Module", IEEE Transactions on Power Electronics, DOI : 10.1109/TPEL.2018.2879845, vol. 34, no 8, pp. 7957-7971, 2019. (Article)

[24] K. Górecki, M. Rogalska, and J. Zarębski, "Parameter estimation of the electrothermal model of the ferromagnetic core", Microelectronics Reliability, DOI: 10.1016/j.microrel.2014.02.003, vol. 54, no 5, pp. 978-984, 2014. (Article)

[25] V. Szekely, "Identification of RC networks by deconvolution: chances and limits", IEEE Transactions on Circuits and Systems I: Fundamental Theory and Applications, DOI : 10.1109/81.662698, vol. 45, no 3, pp. 244-258, 1998. (Article)

[26] A. Poppe, G. Farkas, V. Szekely, G. Horvath and M. Rencz, "Multi-domain simulation and measurement of power LED-s and power LED assemblies", 22nd Annual IEEE Semiconductor Thermal Measurement And Management Symposium, Dallas, TX, USA, pp. 191-198, 2006. (Conference Paper)

[27] Y. C. Gerstenmaier, W. Kiffe and G. Wachutka, "Combination of thermal subsystems modeled by rapid circuit transformation", 13th International Workshop on

Thermal Investigation of ICs and Systems (THERMINIC), Budapest, Hungary, pp. 115-120, 2007. (Conference Paper)

[28]   G. Ellison, "Thermal computations for electronics: conductive, radiative, and convective air cooling", CRC press, 2010. (Book)

[29]   T. Li, X. Du, C. Zeng, P. Sun and H. Tai, "A quasi-online method of thermal network parameter identification for IGBT modules", IEEE Energy Conversion Congress and Exposition (ECCE), Milwaukee, WI, USA, pp. 1-6, 2016. (Conference Paper)

[30]   K. L. Pandya and W. McDaniel, "A simplified method of generating thermal models for power MOSFETs", the 18th Annual IEEE Semiconductor Thermal Measurement and Management Symposium. Proceedings (Cat.No.02CH37311), San Jose, CA, USA, pp. 83-87, 2002. (Conference Paper)

[31]   G. L. Skibinski and W. A. Sethares, "Thermal parameter estimation using recursive identification", IEEE Transactions on Power Electronics, DOI : 10.1109/IAS.1990.152397, vol. 6, no 2, pp. 228-239, 1991. (Article)

[32]   C. Negrea, P. Svasta and M. Rangu, "Electro-thermal modeling of power LED using SPICE circuit solver", 35th International Spring Seminar on Electronics Technology, Bad Aussee, Austria, pp. 329-334, 2012. (Conference Paper)

[33]   V. Roberge, M. Tarbouchi and G. Labonte, "Comparison of Parallel Genetic Algorithm and Particle Swarm Optimization for Real-Time UAV Path Planning", IEEE Transactions on Industrial Informatics, DOI : 10.1109/TII.2012.2198665, vol. 9, no 1, pp. 132-141, 2013. (Article)

[34]   S. Vadi, F. B. Gurbuz, S. Sagiroglu and R. Bayindir, "Optimization of PI Based Buck-Boost Converter by Particle Swarm Optimization Algorithm", 9th International Conference on Smart Grid (icSmartGrid), Setubal, Portugal, pp. 295-301, 2021. (Conference Paper)

[35]   G. A. Ajenikoko, "A genetic algorithm approach for optimal distribution system network reconfiguration", International Journal of Smart Grid (ijSmartGrid), vol. 1, no. 1, pp. 34-41, 2017. (Article)

[36]   S. Korjani, M. Porru, A. Serpi and A. Damiano, "A genetic algorithm for the definition of nodal load time evolutions in micro grids assessment," IEEE International Conference on Renewable Energy Research and Applications (ICRERA), Birmingham, UK, pp. 633-638, doi: 10.1109/ICRERA.2016.7884412, 2016. (Conference paper)

[37]   I. G. Adebayo, M. A. Bhaskar, A. A. Yusuff and A. A. Jimoh, "Optimal location identification of FACTS devices through genetic algorithm and the network structural characteristics techniques," IEEE International Conference on Renewable Energy Research and Applications (ICRERA), Birmingham, UK, pp. 778-782, doi: 10.1109/ICRERA.2016.7884442, 2016. (Conference paper)

[38]   O. Guenounou, A. Belkaid, I. Colak, B. Dahhou and F. Chabour, "Optimization of Fuzzy Logic Controller Based Maximum Power Point Tracking Using Hierarchical Genetic Algorithms", 9th International Conference on Smart Grid (icSmartGrid), Setubal, Portugal, pp. 207-211, 2021. (Conference Paper)

[39]   G. M. Gilbert, N. Shililiandumi, and H. Kimaro, "Evolutionary Approaches to Fog Node Placement in LV Distribution Networks", International Journal of Smart Grid (ijSmartGrid), vol. 5, no 1, pp. 1-14, (2021). (Article)

[40]   M. S. Chaouche, H. Houassine, S. Moulahoum and I. Colak, "Finite element method to construct a lumped parameter ladder network of the transformer winding," IEEE 6th International Conference on Renewable Energy Research and Applications (ICRERA), San Diego, CA, USA, pp. 1092-1096, 2017. (Conference paper)

[41]   H. Ye, M. Lin, and C. Basaran, "Failure modes and FEM analysis of power electronic packaging", Finite Elements in Analysis and Design, DOI: 10.1016/S0168-874X(01)00094-4, vol. 38, no 7, pp. 601-612, 2002. (Article)

[42]   B. Tian, Z. Wang and W. Qiao, "Study on case temperature distribution for condition monitoring of multi die IGBT modules", IEEE Applied Power Electronics Conference and Exposition-APEC, p. 2568, 2014. (Conference Paper)

[43]   Y. Yu, T. T. Lee and V. A. Chiriac, "Compact Thermal Resistor-Capacitor-Network Approach to Predicting Transient Junction Temperatures of a Power Amplifier Module", IEEE Transactions on Components, Packaging and Manufacturing Technology, DOI : 10.1109/TCPMT.2012.2198885, vol. 2, no 7, pp. 1172-1181, 2012. (Article)

[44]   K. Górecki and J. Zarębski, "Modeling the Influence of Selected Factors on Thermal Resistance of Semiconductor Devices", IEEE Transactions on Components, Packaging and Manufacturing Technology, DOI: 10.1109/TCPMT.2013.2290743, vol. 4, no 3, pp.421-428, 2014. (Article)

[45]   P. E. Bagnoli, C. Casarosa, E. Dallago and M. Nardoni, "Thermal resistance analysis by induced transient (TRAIT) method for power electronic devices thermal characterization. II. Practice and experiments", IEEE Transactions on Power Electronics, DOI : 10.1109/63.728349, vol. 13, no 6, pp. 1220-1228, 1998. (Article)

[46]   M. Rencz and V. Szekely, "Dynamic thermal multiport modeling of IC packages", IEEE Transactions on Components and Packaging Technologies,

DOI : 10.1109/6144.974946, vol. 24, no 4, pp. 596-604, 2001. (Article)

[47] R. Wu, H. Wang, K. B. Pedersen, K. Ma, P. Ghimire, F. Iannuzzo, and F. Blaabjerg, "A temperature-dependent thermal model of igbt modules suitable for circuit-level simulations", IEEE Transactions on Industry Applications, DOI : 10.1109/TIA.2016.2540614, vol. 52, no 4, pp. 3306–3314, 2016. (Article)

[48] J. Davidson, D. Stone, and M. Foster, "Required cauer network order for modeling of thermal transfer impedance", Electronics Letters, 10.1049/el.2013.3426, vol. 50, no 4, pp. 260–262, 2014. (Article)

[49] Infineon, "Semiconductor and system solutions-infineon technologies, "http://www.infineon.com/cms/en/product/power/igbt/igbt-module, [Online; accessed 18-August-2021].

[50] SEMIKRON, "Power modules and systems," http://www.semikron.com, [Online; accessed 18-August-2021].

[51] B. Yang, J. Wang, X. Zhang, T. Yu, W. Yao, H. Shu, and L. Sun, "Comprehensive overview of meta-heuristic algorithm applications on PV cell parameter identification", Energy Conversion and Management, DOI: 10.1016/j.enconman.2020.112595; vol. 208, p. 112595, 2020. (Article)

[52] X. Lü, Y. Wu, J. Lian, Y. Zhang, C. Chen, P. Wang, and L. Meng, "Energy management of hybrid electric vehicles: A review of energy optimization of fuel cell hybrid power system based on genetic algorithm", Energy Conversion and Management, vol. 205, p. 112474, 2020. (Article)

[53] W. Tang, Q. Wu, and Z. Richardson, "Equivalent heat circuit based power transformer thermal model", IEE proceedings-electric power applications, vol. 149, no 2, pp. 87–92, 2002. (Conference paper)

[54] O. Alavi, M. Abdollah, and A. H. Viki, "Assessment of thermal network models for estimating igbt junction temperature of a buck converter", the 8th Power Electronics, Drive Systems & Technologies Conference (PEDSTC), Mashhad, Iran, pp. 102–107,2017. (Conference paper)

[55] D. Schweitzer, H. Pape, L. Chen, R. Kutscherauer, and M. Walder, "Transient dual interface measurement a new jedec standard for the measurement of the junction-to-case thermal resistance", the 27th Annual IEEE Semiconductor Thermal Measurement and Management Symposium, San Jose, CA, USA, pp. 222–229, 2011 . (Conference paper)

[56] FLIR, "Flir systems | imagerie thermique, vision nocturne et systems de cameras infrarouges," http://www.flir.fr/home, [Online; accessed 18-August-2021].

[57] R. Ø. Nielsen, J. Due, and S. Munk-Nielsen, "Innovative measuring system for wear-out indication of high power igbt modules", IEEE Energy Conversion Congress and Exposition, Phoenix, AZ, USA, pp.1785–1790, 2011. (Conference paper)

[58] Y. Xiong, X. Cheng, Z. J. Shen, C. Mi, H. Wu, and V. K. Garg, "Prognostic and warning system for power-electronic modules in electric, hybrid electric, and fuel-cell vehicles", IEEE Transactions on Industrial Electronics, DOI : 10.1109/TIE.2008.918399, vol. 55, no 6, pp. 2268–2276, 2008. (Article)

[59] K. Górecki, P. Górecki, and J. Zarębski, "Measurements of parameters of the thermal model of the igbt module", IEEE Transactions on Instrumentation and Measurement, DOI : 10.1109/TIM.2019.2900144, vol. 68, no 12, pp. 4864-4875, 2019. (Article)